

This is a repository copy of *Capacity bounds and estimates for the finite scatterers MIMO wireless channel*.

White Rose Research Online URL for this paper:

<https://eprints.whiterose.ac.uk/653/>

Article:

Burr, A G orcid.org/0000-0001-6435-3962 (2003) Capacity bounds and estimates for the finite scatterers MIMO wireless channel. IEEE Journal on Selected Areas in Communication. pp. 812-818. ISSN 1558-0008

<https://doi.org/10.1109/JSAC.2003.810291>

Reuse

Items deposited in White Rose Research Online are protected by copyright, with all rights reserved unless indicated otherwise. They may be downloaded and/or printed for private study, or other acts as permitted by national copyright laws. The publisher or other rights holders may allow further reproduction and re-use of the full text version. This is indicated by the licence information on the White Rose Research Online record for the item.

Takedown

If you consider content in White Rose Research Online to be in breach of UK law, please notify us by emailing eprints@whiterose.ac.uk including the URL of the record and the reason for the withdrawal request.

Capacity Bounds and Estimates for the Finite Scatterers MIMO Wireless Channel

Alister G. Burr

Abstract—We consider the limits to the capacity of the multiple-input–multiple-output wireless channel as modeled by the finite scatterers channel model, a generic model of the multipath channel which accounts for each individual multipath component. We assume a normalization that allows for the array gain due to multiple receive antenna elements and, hence, can obtain meaningful limits as the number of elements tends to infinity. We show that the capacity is upper bounded by the capacity of an identity channel of dimension equal to the number of scatterers. Because this bound is not very tight, we also determine an estimate of the capacity as the number of transmit/receive elements tends to infinity which is asymptotically accurate.

Index Terms—Finite scatterers channel model, multiple-input–multiple-output (MIMO) capacity.

I. INTRODUCTION

FOLLOWING the work of Telatar [1], Foschini and Gans [2] and many others, it is now well known that multiantenna wireless systems, that is multiple-input–multiple-output (MIMO) channels, can attain capacities many times greater than the Shannon limit for single-input single-output (SISO, or *scalar*) channels. Spectrum efficiencies in the hundreds of bits/s/Hz have been quoted. It is also well-established that these capacities depend critically upon the multipath environment in which the system operates and in particular on the number of resolvable multipath components, their amplitudes, and their spatial distribution.

The original capacity estimates of [1] and [2] were obtained using the *independent Rayleigh-fading model* of the MIMO channel. However, another channel model, which we here call the *finite scatterers model*, has been quite widely used to describe the multipath environment, accounting for each distinct multipath signal. Raleigh and his co-workers [3], [4] have made use of a more complete spatiotemporal version of the model to devise optimum spatiotemporal signalling schemes over a time-dispersive MIMO channel. The *spatial*, or *geometrically-based single-bounce* model [5], [6] is in effect a special case and ray-tracing models [7] are also closely related. The concepts behind the model are in fact implicit in the well-known GWSSUS model of the scalar time-dispersive multipath model [8].

In this paper, we focus on the implications of this model for the capacity of the MIMO wireless channel and derive bounds

and estimates for this capacity. Part of the motivation for this stems from the results of [1] and [2] which suggest that capacity increases indefinitely with the number of transmit/receive antenna elements. (These results were derived from the independent Rayleigh model.) This raises the question of whether this unlimited capacity is available in real scenarios and if not, what factors limit it. The finite scatterers model provides a means of taking into account the specific multipath environment. This will assist in identifying the possible benefits of MIMO systems in practical implementation.

Shiu *et al.* [9] have considered the effect of fading correlation caused by a limited number of scatterers, using a restricted version of the finite scatterers model. They show that capacity is reduced by fading correlation and depends on angular spread, antenna element distribution and spacing, but they do not consider the effect of number of scatterers. Similarly, Chuah *et al.* [10] show that in correlated fading capacity continues to increase with number of antennas, but less rapidly than in independent fading. Again, however, they do not consider a finite number of multipath components. Loyka [13] also considers the effect of correlated fading, but does not relate this to the multipath environment. Raleigh and Cioffi in the work cited above [4] show that the *capacity slope* [variation of capacity with signal-to-noise ratio (SNR)] is limited by the number of scatterers, but do not bound the capacity itself. Boelskei *et al.* [11] use a model similar to but more general than ours, which considers clusters of scatterers rather than individual discrete scatterers. Their focus, however, is on OFDM systems and they do not bring out the results given here. Sayeed [12] describes an interesting and related model which incorporates the effect of limited multipath, but does not explicitly model individual scatterers. Gesbert *et al.* [18] describe what is effectively a double-bounce scattering model, which can exhibit interesting properties described as “pinhole” effects and some features of which can be accounted for in our model in the manner described in the next section. Müller [14] uses a new theory of random matrices to derive the capacity in the limit as number of antennas and number of scatterers tends to infinity, but maintaining a constant ratio.

In this paper, we will consider the capacity of a MIMO channel with a finite number of scatterers, a case which is well described by the finite scatterers model. The number of transmit/receive elements will be allowed to tend to infinity. For this reason, we will use a channel normalization, different from that of [1] and [2], which compensates for the increasing array gain which would otherwise necessarily result in infinite capacity for infinite numbers of receive elements. (Our normalization may also be regarded as an alternative definition of SNR.)

Manuscript received April 30, 2002; revised November 19, 2002. This paper was presented in part at Antennas and Propagation 2000 (AP2000), Davos, Switzerland, April 2000.

The author is with the Department of Electronics, University of York, York YO10 5DD, U.K. (e-mail: alister@ohm.york.ac.uk).

Digital Object Identifier 10.1109/JSAC.2003.810291

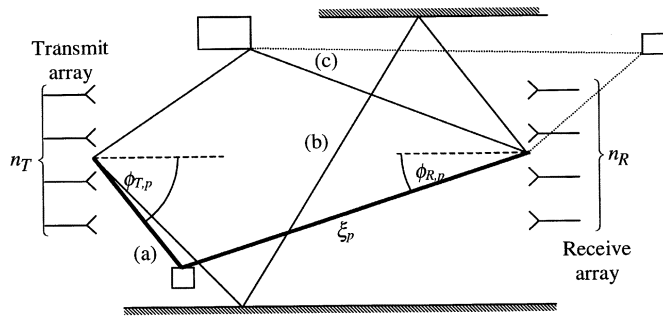


Fig. 1. Concept of the finite scatterers channel model, illustrating (a) typical single scattered path p , (b) reflected path, and (c) double scattered path.

The next section, then, describes the finite scatterers model as we will apply it, including this channel normalization, pointing out also the limits of its applicability in practical scenarios. We then derive an upper bound on the capacity of the channel and show that a similar bound applies to all channels normalized as we have described. We also derive capacity estimates which are asymptotically accurate as the number of antennas tends to infinity.

II. FINITE SCATTERERS CHANNEL MODEL

The concept of the finite scatterers model is illustrated in Fig. 1. Its fundamental assumption is that the signal travels from transmitter to receiver via a number, normally finite, of discrete paths, referred to as *multipath components*, or simply *multipaths*. These are treated according to ray-optical concepts, although diffraction can also be treated using concepts from the geometrical theory of diffraction (GTD) [15]. Fig. 1 illustrates some of the possible mechanisms, including scattering from a single scatterer [path (a)] and multiple reflections [path (b)]. Path (c) in Fig. 1 includes both single scattering and double scattering: i.e., further scattering of the scattered signal from a second scatterer.

Note that this model describes the radio environment separately from the antenna arrays, unlike the independent Rayleigh-fading model, in which the propagation between transmit/receive antenna elements are described directly. Thus, the model can be used to predict propagation between any pair of antenna arrays and does not require array sizes or geometries to be defined *a priori*. In this paper, we take an idealized view of the antenna elements, treating transmit elements as ideal uncoupled isotropic radiators and assuming that receive elements sample the electromagnetic field without perturbing it and similarly are isotropic and uncoupled. For any given real antenna array it is usually possible to allow for deviations from this ideal by multiplying by appropriate transformation matrices [16]. We also assume that the sources and scatterers are distant from one another and from the receiving array in comparison with the dimensions of the array, which is equivalent to assuming that we operate in the far field of both scatterers and sources.

In the finite scatterers model, each path is indexed by an integer p and has a defined angle of departure (AoD) from the transmitting array $\phi_{T,p}$, angle of arrival (AoA) at the receiving array $\phi_{R,p}$, and path gain ξ_p defined as the ratio of the electric/magnetic field at the location of the receiving array to that

at the transmitting array. In accordance with the term “finite,” we will for the most part in this paper assume that there is a finite number of multipaths, n_S , so that $p \in [1, n_S]$. However, the model could be extended to an infinite number, with $p \in [1, \infty]$. In general, each multipath also has a time delay τ_p , but in this paper we will neglect this, which is equivalent to assuming that the signal bandwidth is narrow compared with the overall coherence bandwidth of the channel.

This model fits well with the spatial or “single-bounce” channel models [5], [6], and with ray-tracing models. In the former, the AoA and AoD are defined by the scatterer location [as in path (a) in Fig. 1]; in the latter there is a set of distinct paths which can be traced out [as in path (b) in Fig. 1], although in many cases there may be a potentially infinite number of such paths. However, multiply-scattered paths like (c) in Fig. 1 pose a potential problem for the model, in that they have a single AoD but two (or more) AoAs. This problem will be dealt with here by treating such paths as a pair of components, which in the case illustrated would have the same AoDs but different AoAs. (Note that due to reciprocity it is equally possible to have multiple AoDs with the same AoA.) However, we will see later that such paths raise particular issues for channel capacity. Channel models like that of [11], which deal with clusters of scatterers rather than individual scatterers, could also in principle be covered, by grouping many scatterers into a single cluster, but this would not be very illuminating compared with the approach of [11]. However, space does not allow a more detailed examination here.

The signals applied to the transmit elements are described as a length n_T column vector and similar the received signals as a length n_R column vector, where n_T and n_R are the number of transmit and receive antenna elements, respectively. Let the response of the receive array to a signal from AoA ϕ_R be $\psi_R(\phi_R)$. Similarly, we can express the signal transmitted in a direction ϕ_T as $\psi_T^T(\phi_T) \cdot \mathbf{s}$, where \mathbf{s} is the vector of signals at the transmitter. Hence, the signal transmitted at the AoD of the p th multipath $\phi_{T,p}$ is $\psi_T^T(\phi_{T,p}) \cdot \mathbf{s}$, where $(\cdot)^T$ denotes transpose and the corresponding received vector \mathbf{r} is $\psi_R(\phi_{R,p}) \xi_p \psi_T^T(\phi_{T,p}) \cdot \mathbf{s}$. Hence, the complete received signal from all paths, neglecting noise at the receiver is

$$\mathbf{r} = \sum_{p=1}^{n_S} \psi_R(\phi_{R,p}) \xi_p \psi_T^T(\phi_{T,p}) \cdot \mathbf{s} = \Psi_R \Xi \Psi_T^T \mathbf{s} \quad (1)$$

where Ψ_T and Ψ_R are, respectively, $(n_T \times n_S)$ and $(n_R \times n_S)$ matrices whose columns are $\psi_R(\phi_{R,p})$ and $\psi_T^T(\phi_{T,p})$, $p = 1 \cdots n_S$. Ξ is an $(n_S \times n_S)$ diagonal matrix whose diagonal elements are ξ_p , $p = 1 \cdots n_S$.

Where it is necessary to assume any particular array geometry in this paper we will suppose that both transmit and receive arrays are linear with constant element spacings l_T , l_R , respectively. Then, the transmit and receive antenna response vectors referred to above are given by

$$\psi_{\{T,R\}}(\phi) = \left\{ \exp \left(2\pi j \frac{i l_{\{T,R\}}}{\lambda} \sin(\phi) \right) \right. \\ \left. i = 0 \cdots n_{\{T,R\}} - 1 \right\}^T \quad (2)$$

where λ here is the wavelength.

Including noise, the relationship of receive vector \mathbf{r} to transmit vector \mathbf{s} is commonly written

$$\mathbf{r} = \mathbf{H}\mathbf{s} + \mathbf{n} \quad (3)$$

where \mathbf{H} is the channel matrix and \mathbf{n} is the vector of thermal noise. We assume that each element of the noise vector is a complex Gaussian variable of power $\overline{|n_i|^2} = N$, $i = 0 \cdots n_R - 1$.

Performance is evaluated, as in most other works, in terms of the ratio of total transmit power S to noise power per receiver N . In this paper, in common with works such as [14] and [17], but unlike [1] and [2], we assume a normalization which ensures that the total receive power is the same as total transmit power, averaged over random instances of the channel matrix, that is

$$\sum_{i=1}^{n_R} \sum_{k=1}^{n_T} \overline{|H_{ik}|^2} = n_T. \quad (4)$$

This has the effect of separating the array gain, due purely to the increase in antenna gain from more antenna elements, from any gain due to MIMO effects specifically. It is also equivalent to defining the SNR as the ratio of average total **received** signal power to noise power per element. Such a normalization is necessary here to allow us to consider limiting cases as the number of transmit/receive elements tends to infinity. In these cases, the approach used in [1] and [2] would result in infinite receive power and, hence, no limit could be obtained.

Substituting from (1) into (4) we have that in order to maintain this normalization

$$\begin{aligned} \sum_{i=1}^{n_T} \sum_{k=1}^{n_R} \overline{|H_{ik}|^2} &= \sum_{i=1}^{n_T} \sum_{k=1}^{n_R} \sum_{p=1}^{n_S} \overline{|\psi_{R,i}(\phi_{R,p}) \xi_p \psi_{T,k}^*(\phi_{T,p})|^2} \\ &= \sum_{i=1}^{n_T} \sum_{k=1}^{n_R} \sum_{p=1}^{n_S} \overline{|\xi_p|^2} = n_T \\ \therefore \sum_{p=1}^{n_S} \overline{|\xi_p|^2} &= \frac{1}{n_R} \end{aligned} \quad (5)$$

assuming that the transmit and receive elements are isotropic and, hence, the terms of $\Psi_{\{T,R\}}$ have unit magnitude.

III. CAPACITY AND CAPACITY BOUNDS

A. Capacity of the MIMO Channel

We determine the capacity of the MIMO channel in the same way as [1] and [2]: we decompose the channel into a set of orthogonal eigenmodes, using the singular value decomposition, then calculate the sum of the capacities of the uncoupled channels formed by these modes. We may write

$$\mathbf{H} = \mathbf{V}\mathbf{\Lambda}\mathbf{U}^H \quad (6)$$

where \mathbf{U} and \mathbf{V} are unitary matrices whose columns are the eigenvectors at transmitter and receiver respectively, the superscript \mathbf{H} denotes the Hermitian, or conjugate transpose and $\mathbf{\Lambda}$ is a diagonal matrix whose diagonal elements are the square roots of the eigenvalues of $\mathbf{H}^H\mathbf{H}$ (also known as the *singular values*). The total channel capacity, assuming that the channel is unknown at the transmitter, can then be obtained [1], [2] as

$$C = \sum_{i=1}^n C(\lambda_i) = W \sum_{i=1}^n \log_2 \left(1 + \frac{S\lambda_i}{n_T N} \right) \quad (7)$$

where the λ_i 's are the eigenvalues and W is the channel bandwidth. (Note that when λ occurs without a subscript it refers to wavelength; with a subscript it is an eigenvalue.) As noted above, we assume here that W is small compared with the channel coherence bandwidth, i.e

$$W \ll \delta_c = \frac{1}{\sqrt{\sum_{p=1}^{n_S} |\xi_p|^2 (\tau_p - \bar{\tau})^2}}. \quad (8)$$

Equation (6) assumes that the channel is unknown at the transmitter and, hence, that the transmit power S is equally distributed between the eigenmodes. $C(\lambda_i)$ in (7) is the capacity due to the i th eigenmode.

B. Upper Bound on Average Channel Capacity

In this section, we derive an upper bound on average capacity which applies to any MIMO channel for which the normalization of (4) holds. The sum of the eigenvalues of a matrix is given by its trace, that is

$$\sum_{i=1}^{n_T} \lambda_i = \text{trace}(\mathbf{H}^H\mathbf{H}) = \sum_{i=1}^{n_T} \sum_{k=1}^{n_R} |H_{ij}|^2 \quad (9)$$

The function $C(\lambda_i)$ in (6) is monotonically increasing and convex, that is, its slope is positive but decreases monotonically with increasing argument. Let $C_0 = n_T C(\lambda_0)$. Then, making use of the convexity property

$$C(\lambda_i) \leq C(\lambda_0) + \frac{dC(\lambda_0)}{d\lambda_0} (\lambda_i - \lambda_0) \quad (10)$$

with equality if and only if $\lambda_i = \lambda_0$. Then, the average capacity

$$\begin{aligned} \bar{C} &= \sum_{i=1}^{n_T} \int_0^\infty p(\lambda_i) C(\lambda_i) d\lambda_i \\ &\leq \sum_{i=1}^{n_T} \int_0^\infty p(\lambda_i) \left(C(\lambda_0) + (\lambda_i - \lambda_0) \frac{dC(\lambda_0)}{d\lambda_0} \right) d\lambda_i \\ &= \sum_{i=1}^{n_T} \left[C(\lambda_0) + \frac{dC(\lambda_0)}{d\lambda_0} \left(\int_0^\infty \lambda_i p(\lambda_i) d\lambda_i - \lambda_0 \right) \right] \\ &= \sum_{i=1}^{n_T} \left[C(\lambda_0) + \frac{dC(\lambda_0)}{d\lambda_0} (\bar{\lambda}_i - \lambda_0) \right] \\ &= n_T C(\lambda_0) + \frac{dC(\lambda_0)}{d\lambda_0} \left(\sum_{i=1}^{n_T} \bar{\lambda}_i - n_T \lambda_0 \right). \end{aligned} \quad (11)$$

If $\sum_{i=1}^{n_T} \bar{\lambda}_i = n_T \lambda_0$, that is λ_0 is the average of the eigenvalues, then the second term in this result is zero. From (4) and (9)

$$\sum_{i=1}^{n_T} \bar{\lambda}_i = \sum_{i=1}^{n_T} \sum_{k=1}^{n_R} |H_{ij}|^2 = n_T \quad (12)$$

and, therefore, the average is unity. Then

$$\bar{C} = n_T C(\lambda_0) = n_T C(1) = n_T W \log_2 \left(1 + \frac{S}{n_T N} \right). \quad (13)$$

This is the capacity of the $(n_T \times n_T)$ identity channel: that is, the channel whose matrix $\mathbf{H} = \mathbf{I}_{n_T}$.

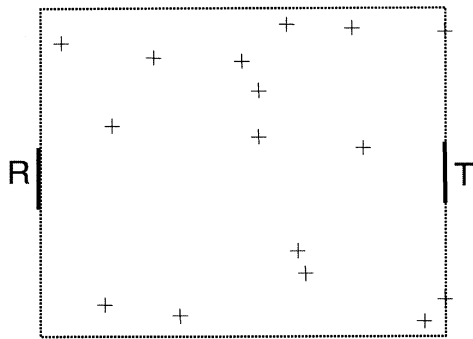


Fig. 2. Simulation of a spatial, single-bounce channel model.

It is clear from the decomposition given in (1) and is also shown in [4], that the rank of \mathbf{H} is upper bounded by

$$n \leq \min(n_T, n_S, n_R) \quad (14)$$

That is, if $n_T, n_R > n_S$ it is the number of multipaths that limits the rank. Moreover, paths like (c) in Fig. 1, which we have treated as two multipaths, in fact contribute only once to the rank, because either Ψ_T or Ψ_R has a repeated column. Hence, n is upper bounded by the number of multipaths which have distinct angles of both arrival and departure.

If $n < n_T$, the number of nonzero eigenvalues is n rather than n_T and, hence, (11) may be rewritten as

$$\begin{aligned} \bar{C} &= \sum_{i=1}^n \int_0^{\infty} p(\lambda_i) C(\lambda_i) d\lambda_i \\ &\leq nC(\lambda_0) + \frac{dC(\lambda_0)}{d\lambda_0} \left(\sum_{i=1}^n \bar{\lambda}_i - n\lambda_0 \right). \end{aligned} \quad (15)$$

The second term is zero if

$$\begin{aligned} n\lambda_0 &= \sum_{i=1}^n \bar{\lambda}_i = n_T \\ \lambda_0 &= \frac{n_T}{n}. \end{aligned} \quad (16)$$

Then

$$\bar{C} \leq nC\left(\frac{n_T}{n}\right) = nW \log_2 \left(1 + \frac{S}{nN} \right) \quad (17)$$

which is the capacity of an $(n \times n)$ identity channel.

C. Simulation of Finite Scatterers Channel

A simulation of a simple spatial, single-bounce model has been established in order to check the tightness of the bound of (17) in some very simple cases.

We assume that a fixed number of scatterers are distributed within a square region, as shown in Fig. 2. The distribution within the region is random with uniform density. We place uniform linear, $\lambda/2$ -spaced transmitting and receiving antenna arrays on opposite sides of the square, as shown by “T” and “R” in the figure. For a uniform linear array (ULA) the transmit and receive response vectors are given by (2). Note that for a $\lambda/2$ -spaced ULA the response vector depends on $\sin(\phi)$; the

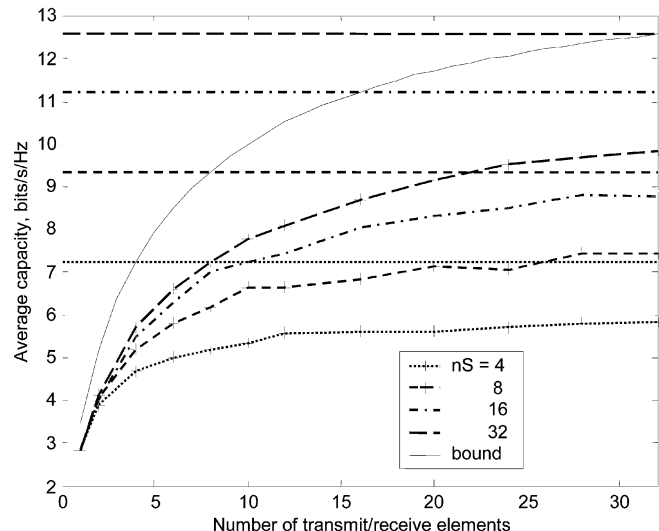


Fig. 3. Simulation (“+”) and bounds (solid lines) for capacity of spatial channel, SNR 10 dB, equal numbers of transmit/receive elements, i.i.d path gains. Colored lines are bounds derived from $(n_S \times n_S)$ identity channel, black line is bound for $(n_T \times n_T)$ channel.

advantage of this distribution of scatterers is that it results in an approximately uniform density of angles of arrival and departure for the multipaths. We further assume that the path gains $\xi_p, p = 1 \dots n_S$ are independent complex Gaussian variables, i.e., that the multipaths are independently Rayleigh fading, as in the conventional GWSSUS model [8]. Initially, we assume that all paths have the same root-mean-square (rms) gain and, hence, from (5)

$$\overline{|\xi_p|^2} = \frac{1}{n_R n_S}. \quad (18)$$

Monte Carlo simulations have been performed for a given number of scatterers, assigning random locations to the scatterers and random complex Gaussian values for the path gains. AoAs and AoDs were then computed from the geometry of Fig. 2, from which the channel matrix \mathbf{H} was computed using (1), (2), and (18). Hence, capacity was calculated by performing a singular value decomposition on \mathbf{H} and using (7). A capacity distribution is obtained by repeating this procedure for many randomly chosen instances of scatterer locations and path gains.

Fig. 3 shows the results of this simulation for a range of receive/transmit antenna sizes and numbers of scatterers. In all cases, the number of transmit and receive elements were the same. The SNR as defined above is 10 dB. The number of random instances for each point is 500. The overall bound based on (13) and the bounds for various numbers of scatterers are also shown. We note that the bounds are not very tight, even asymptotically as the number of antenna elements increases.

Moreover, in Fig. 3, we assume that the mean amplitudes of the signals from all scatterers is the same, neglecting variations in path loss and effective scatterer cross section. In Fig. 4, we include the effect of log-normal shadow fading on each path, in addition to the Rayleigh fading for eight scatterers. We note that the bound is still less tight, even though we have ensured that the normalization of (4) still applies.

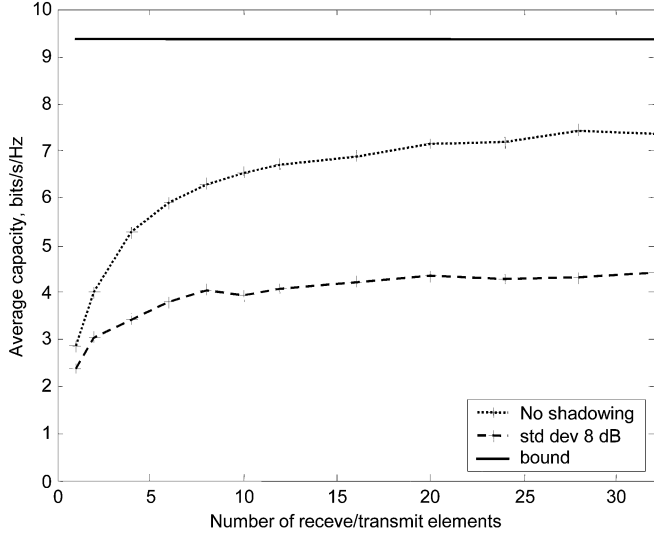


Fig. 4. Simulation of capacity of spatial channel, SNR 10 dB, eight scatterers, with and without log-normal fading compared with bound for eight scatterers.

D. Estimate of Asymptotic Capacity Distribution

In this section, we attempt to overcome the slackness of the bound obtained in Section III-B by deriving an estimate of the capacity which, we will argue, is asymptotically accurate as n_R , $n_T \rightarrow \infty$. We will assume that linear, $\lambda/2$ -spaced arrays are used at both transmitter and receiver, although it is to be expected that the estimate will still be valid for most other array geometries provided the element spacing remains constant as the array size increases.

Consider the matrix $\mathbf{H}^H \mathbf{H}$ whose eigenvalues are the squares of the singular values referred to in Section III-A. Using (1)

$$\mathbf{H}^H \mathbf{H} = \Psi_T^* \Xi^H \Psi_R^H \Psi_R \Xi \Psi_T^T. \quad (19)$$

Consider first the innermost product in this expression

$$\Psi_R^H \Psi_R = \mathbf{R}_R = \{R_{R,ik}\}, R_{R,ik} = \psi_R^H(\phi_{R,i}) \cdot \psi_R(\phi_{R,k}). \quad (20)$$

Using (2)

$$\begin{aligned} R_{R,ik} &= \psi_R^H(\phi_{R,i}) \cdot \psi_R(\phi_{R,k}) \\ &= \sum_{m=0}^{n_R-1} \exp\left(-2\pi j \frac{ml_R}{\lambda} \sin(\phi_{R,i})\right) \\ &\quad \cdot \exp\left(2\pi j \frac{ml_R}{\lambda} \sin(\phi_{R,k})\right) \\ &= \sum_{m=0}^{n_R-1} \exp\left(2\pi j \frac{ml_R}{\lambda} (\sin(\phi_{R,k}) - \sin(\phi_{R,i}))\right). \end{aligned} \quad (21)$$

If $l_R/\lambda(\sin(\phi_{R,k}) - \sin(\phi_{R,i}))$ is an integer (in practice the probability of this is vanishingly small unless $\phi_{R,k} = \phi_{R,i}$), then $R_{R,ik} = n_R$. Otherwise it is bounded as $n_R \rightarrow \infty$. If $\phi_{R,i} \neq \phi_{R,k}, \forall i, k, i \neq k$ then $\mathbf{R}_R \rightarrow n_R \mathbf{I}, n_R \rightarrow \infty$. This will generally be the case unless paths such as (c) in Fig. 1 exist. Using this result in (19), extending it to $\mathbf{R}_T = \Psi_T^H \Psi_T$ and using the fact that Ξ is diagonal, we have

$$\mathbf{H}^H \mathbf{H} = \Psi_T^* \Xi^H \Psi_R^H \Psi_R \Xi \Psi_T^T \xrightarrow{n_R \rightarrow \infty} n_R \Psi_T^* \Xi^H \Psi_T^T \xrightarrow{n_T \rightarrow \infty} n_R n_T \Xi^H \Xi. \quad (22)$$

$\Xi^H \Xi$ is a diagonal matrix whose diagonal elements are the multipath power gains, $|\xi_p|^2, p \in [1, n_S]$. The eigenvalues of a diagonal matrix are simply the diagonal elements and, hence, $n_R n_T \Xi^H \Xi$ has n_S eigenvalues, with values $\lambda_i = n_T n_R |\xi_i|^2, i = 1 \dots n_S$. Substituting these values into (7) gives an estimate of the capacity of the channel as the number of antenna elements, $n_T, n_R \rightarrow \infty$

$$C = W \sum_{i=1}^{n_S} \log_2 \left(1 + \frac{n_R n_S |\xi_i|^2}{N} \right). \quad (23)$$

We have shown that this is asymptotically accurate provided all paths have distinct angles of arrival and departure. We now take the case in which some paths do not have distinct angles of arrival. If for some $i, k, i \neq k, \phi_{R,i} = \phi_{R,k}$, then \mathbf{R}_R will have a pair of off-diagonal elements $R_{R,ik} = R_{R,ki} = n_R$. We then find that $n_R n_T \Xi^H \Xi$ takes the form

$$\frac{n_T}{n_S} \begin{bmatrix} |\xi_1|^2 & 0 & 0 & \dots & 0 & \dots & 0 \\ 0 & |\xi_2|^2 & 0 & \dots & 0 & \dots & 0 \\ & & \ddots & & & & \\ 0 & 0 & 0 & |\xi_i|^2 & 0 & \xi_i^* \xi_k & 0 \\ \vdots & \vdots & \vdots & 0 & \ddots & \vdots & \vdots \\ 0 & 0 & \xi_i \xi_k^* & 0 & |\xi_k|^2 & \vdots & 0 \\ \vdots & \vdots & \vdots & \dots & \dots & \ddots & \vdots \\ 0 & 0 & 0 & \dots & 0 & \dots & |\xi_{n_S}|^2 \end{bmatrix}. \quad (24)$$

The eigenvalues of this are

$$\frac{n_T}{n_S} \left\{ \left\{ |\xi_p|^2, p = 1 \dots n_S, p \neq i, k \right\}, |\xi_i|^2 + |\xi_k|^2 \right\}. \quad (25)$$

In other words, the two paths which have the same AoA contribute to a single eigenmode whose eigenvalue is given by the sum of the two path gains. It is easy to see that the same will apply to two paths which have the same AoD at the transmitter.

Assuming that the multipaths are subject to independent Rayleigh fading, we can obtain the mean capacity from (23)

$$\begin{aligned} E\{C\} &= W \sum_{i=1}^{n_S} \int_0^\infty \log_2 \left(1 + \frac{n_R n_S |\xi_i|^2}{N} \right) \\ &\quad \cdot \frac{1}{X_i} \exp\left(-\frac{|\xi_i|^2}{X_i}\right) d|\xi_i|^2 \\ &= \frac{W}{\ln 2} \sum_{i=1}^{n_S} \exp\left(-\frac{N}{n_R n_S X_i}\right) \Gamma\left(0, \frac{N}{n_R n_S X_i}\right) \end{aligned} \quad (26)$$

where X_i denotes the mean (power) gain of the i th multipath and $\Gamma(0, x)$ denotes the incomplete Gamma function, defined as

$$\Gamma(0, x) = \int_x^\infty \frac{\exp(-t)}{t} dt. \quad (27)$$

If all paths have equal mean power gains, then from (5) $X_i = 1/(n_S n_R), i = 1 \dots n_S$ and (26) becomes

$$E\{C\} = \frac{n_S W}{\ln 2} \exp\left(-\frac{N n_S}{S}\right) \Gamma\left(0, \frac{N n_S}{S}\right). \quad (28)$$

For $n_S = 8$, SNR 10 dB gives 7.98 bits/s/Hz. On the assumption of log-normal fading, standard deviation 8 dB, in addition to the Rayleigh, as in Fig. 4, the mean capacity is 4.5 bits/s/Hz.

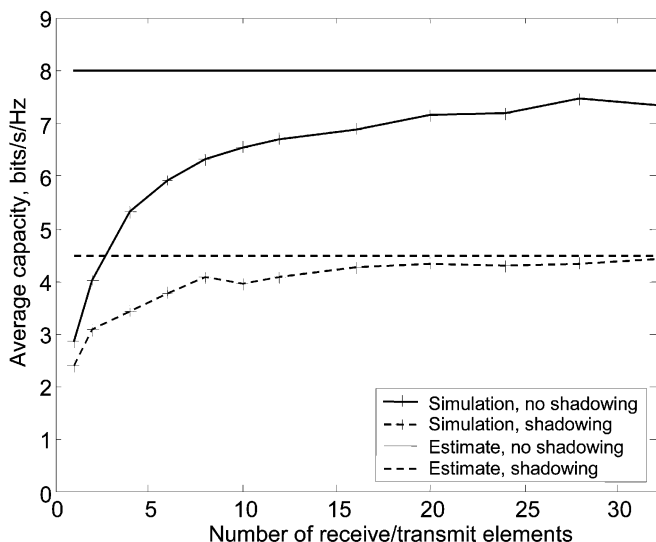


Fig. 5. Simulation results of Fig. 4 compared with asymptotic estimates from Section III-D.

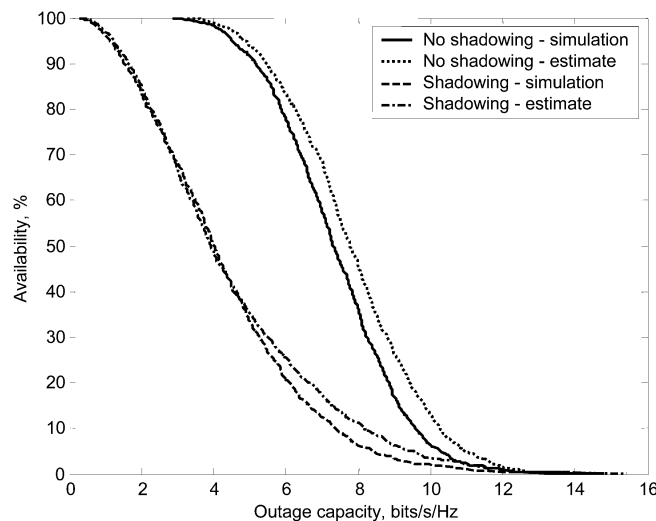


Fig. 6. Cumulative distribution function of capacity with eight scatterers and 32 transmit/receive antenna elements, SNR 10 dB, compared with estimate, with and without log-normal shadow fading, standard deviation 8 dB.

Fig. 5 compares the simulation results shown in Fig. 4 with these asymptotic estimates, showing that they are much closer than the bound of Section III-B, especially in the log-normal fading case. Fig. 6 shows the distributions of capacity, from which the capacity for given availability (outage capacity) can be calculated. We observe that the distribution, as well as the mean, is very close to the estimate.

We may note that neither the bounds nor the asymptotic estimates depend on the antenna element spacing. Fig. 7 compares the results of simulations with different element spacings with the asymptotic estimate. We observe that in the limit they appear to be approaching the same bound, although with spacing less than $\lambda/2$ they do so more slowly. Larger spacings, however, have little effect on capacity in this case because in the scenario simulated the angle spread at both transmitter and receiver is large. This result confirms that with a limited number

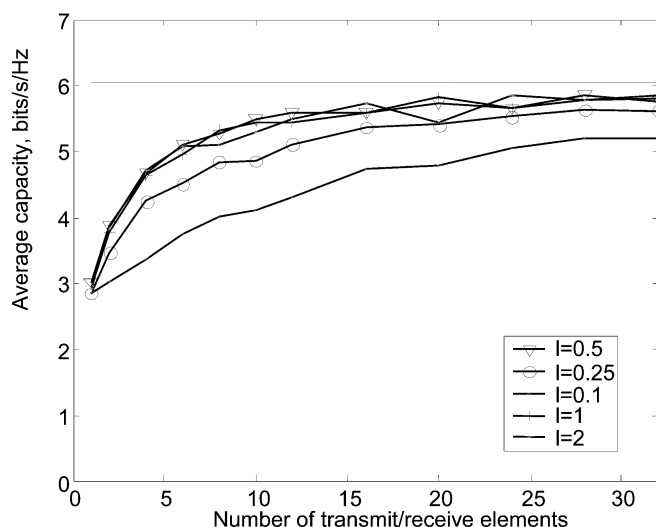


Fig. 7. Capacity with linear transmit/receive arrays with different element spacings (as a fraction of a wavelength) compared with asymptotic estimate.

of scatterers it is not possible to increase the limiting capacity by increasing the element spacing.

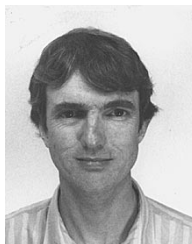
IV. CONCLUSION

We have analyzed the capacity of the finite scatterers channel model and have shown that under a channel normalization which compensates for receive array gain, average capacity is upper bounded by the capacity of an identity channel of dimension equal to the number of multipath components which have distinct angles of departure/arrival at the transmit/receive antenna. However, having compared this bound with the result of a simulation of a simple scenario, we find that it is not tight and, therefore, we derive an estimate of the capacity which is asymptotically accurate as the number of receive/transmit antenna elements tends to infinity. This is much closer to the simulation results in terms of average capacity and we note also that it can estimate the probability distribution function of the capacity quite accurately. It can also allow for the case where multipath components have different amplitudes, which is illustrated here by assuming log-normal fading, as well as Rayleigh fading of the components.

REFERENCES

- [1] I. E. Telatar. (1995) Capacity of Multi-Antenna Gaussian Channels. AT&T Bell Labs internal report. [Online]. Available: <http://mars.bell-labs.com/cm/ms/what/mars/index.html>
- [2] G. J. Foschini and M. J. Gans, "On limits of wireless communications in a fading environment when using multiple antennas," *Wireless Pers. Commun.*, vol. 6, pp. 311–335, 1998.
- [3] G. G. Raleigh and V. K. Jones, "Multivariate modulation and coding for wireless communication," *IEEE J. Select. Areas Commun.*, vol. 17, pp. 851–866, May 1999.
- [4] G. G. Raleigh and J. M. Cioffi, "Spatio-temporal coding for wireless communication," *IEEE Trans. Commun.*, vol. 46, pp. 357–366, Mar. 1998.
- [5] J. Fuhl, A. F. Molisch, and E. Bonek, "Unified channel model for mobile radio systems with smart antennas," *IEE Proc. Radar Sonar and Navigation*, vol. 145, no. 1, pp. 32–41, 1998.
- [6] P. Petrus, J. H. Reed, and T. S. Rappaport, "Geometrical-based statistical macrocell channel model for mobile environments," *IEEE Trans. Commun.*, vol. 50, pp. 495–502, Mar. 2002.

- [7] S. Loredó, L. Valle, and R. P. Torres, "Accuracy analysis of GO/UTD radio-channel modeling in indoor scenarios at 1.8 and 2.5 GHz," *IEEE Antennas and Propagat. Mag.*, vol. 43, pp. 37–51, Oct. 2001.
- [8] P. A. Bello, "Characterization of randomly time-variant linear channels," *IEEE Trans. Commun. Syst.*, vol. CS-11, pp. 36–393, Dec. 1963.
- [9] D.-S. Shiu, G. J. Foschini, M. J. Gans, and J. M. Kahn, "Fading correlation and its effect on the capacity of multi-element antenna systems," *IEEE Trans. Commun.*, vol. 48, pp. 502–513, Mar. 2000.
- [10] C.-N. Chuah, D. N. Tse, J. M. Kahn, and R. A. Valenzuela, "Capacity scaling in MIMO wireless systems under correlated fading," *IEEE Trans. Inform. Theory*, vol. 48, pp. 637–650, Mar. 2002.
- [11] H. Boelskei, D. Gesbert, and A. J. Paulraj, "On the capacity of OFDM-based spatial multiplexing systems," *IEEE Trans. Commun.*, vol. 50, pp. 225–234, Feb. 2002.
- [12] A. M. Sayeed, "Modeling and capacity of realistic spatial MIMO channels," in *Proc. 2001 IEEE Int. Conf. Acoustics, Speech, Signal Processing*, vol. 4, 2001, May, pp. 2489–2492.
- [13] S. L. Loyka, "Channel capacity of MIMO architecture using the exponential correlation matrix," *IEEE Commun. Lett.*, vol. 5, pp. 369–371, Sept. 2001.
- [14] R. R. Müller, "A random matrix theory of communication via antenna arrays," *IEEE Trans. Inform. Theory*.
- [15] J. B. Keller, "Geometrical theory of diffraction," *J. Opt. Soc. Amer.*, vol. 52, no. 2, pp. 116–130, 1962.
- [16] H. Steyskal and J. S. Herd, "Mutual coupling compensation in small array antennas," *IEEE Trans. Antennas Propagat.*, vol. 38, no. 12, pp. 1971–1975, Dec. 1990.
- [17] N. Chiurtu, B. Rimoldi, and E. Telatar, "Dense multiple antenna systems," in *Proc. ITW 2001*, Cairn, Australia, Sept. 2–7, 2001.
- [18] D. Gesbert, H. Boelskei, D. A. Gore, and A. J. Paulraj, "Outdoor MIMO wireless channels: Models and performance prediction," *IEEE Trans. Commun.*, vol. 50, pp. 1926–1934, Dec. 2002.



Alister G. Burr received the B.Sc. degree from the University of Southampton, Southampton, U.K., and the Ph.D. degree from the University of Bristol, Bristol, U.K., in 1979 and 1984, respectively.

Since 1985, he has been with the Department of Electronics, University of York, York, U.K., where he is now a Professor of communications. His research interests are primarily in modulation and coding techniques for digital wireless communications and especially turbocodes and MIMO techniques. From 1999 to 2000, he undertook a Royal Society Senior Research Fellowship researching space–time codes and MIMO systems and has also held a Visiting Professorship at Vienna University of Technology, Vienna, Austria. He is currently Chair WG1 of the European Programme COST 273: "Toward Mobile Broadband Networks."